Picosecond pulse amplification by coherent wave mixing in silicon

H. J. Eichler, M. Glotz, A. Kummrow, K. Richter, and X. Yang*
Optisches Institut der Technischen Universität Berlin, D-1000 Berlin, Germany
(Received 14 October 1986)

Pulses from Nd:YAG lasers (where YAG represents yttrium aluminum garnet) were amplified up to 20 times by noncollinear mixing with a coherent pump wave in silicon. Amplification of long pulses (about 16 ns) was obtained with intersection angles up to 2° whereas angles larger than 10° are possible with short pulses (50 ps). The effect is theoretically described by self-diffraction at a laser-induced dynamic free-carrier grating.

INTRODUCTION AND SURVEY OF PREVIOUS WORK

Light amplification by coherent two-wave mixing has been investigated in a number of different materials as reviewed, e.g., in Refs. 1 and 2. The amplification is due to energy transfer from a strong pump beam to a weak noncollinear signal beam. This two-wave-mixing process can be explained by formation of a light-induced refractive-index grating which diffracts the pump into the direction of the signal beam. The effect is useful for construction of self-pumped phase-conjugating reflectors and potentially also for low noise image amplification.[2,3]

High two-wave-mixing gains up to 10^4 are possible in photorefractive materials, e.g., $BaTiO_3$ and $KNbO_3$. However, the laser-induced refractive-index gratings in these materials have rather long buildup and decay times of about 1 ms (Ref. 4), so that only amplification of signals with a slow time variation seems possible. Faster response is expected for semiconductors, e.g., Si (Refs. 5 and 6), CdS, CdSe, ZnSe (Ref. 7), and SiC (Ref. 8) with grating decay times about 1 ns.

Pulse amplification in silicon was first demonstrated by Vinetskii *et al.*[5,6] using a Q-switched Nd:glass laser with a 30-ns pulse width. Similar experiments were done also by us, showing that the gain decreased with increasing beam intersection angle θ [Fig. 1(a)]. Amplification of 16-ns pulses was possible only for $\theta \leq 2°$. Such small intersection angles are inconvenient for practical applications. The gain decrease is partially due to shortening of the grating lifetime which is given by free-carrier diffusion and becomes small at large interaction angles, i.e., small grating periods.[9] Theory shows that two-wave-mixing gain is obtainable in silicon, a material with local response, only if the pulse width is sufficiently short compared to the grating decay time.[1] We expected therefore that picosecond pulses would be favorable for two-wave-mixing experiments allowing larger beam intersection angles.

In this work the term "two-wave mixing" is used to describe the experiment where two incident beams interact and exchange energy. The process is called "three-wave mixing" if a third beam is produced due to the interaction. The term two-wave mixing is common to describe beam coupling in photorefractive materials.[1–4] In the nonlinear susceptibility formalism the interaction between two beams with equal frequencies results from a third-order susceptibility. In general, such a susceptibility may couple four independent waves resulting in "four-wave mixing." Since only two or three waves are observable in our experiment, we do not use the term four-wave mixing in this connection.

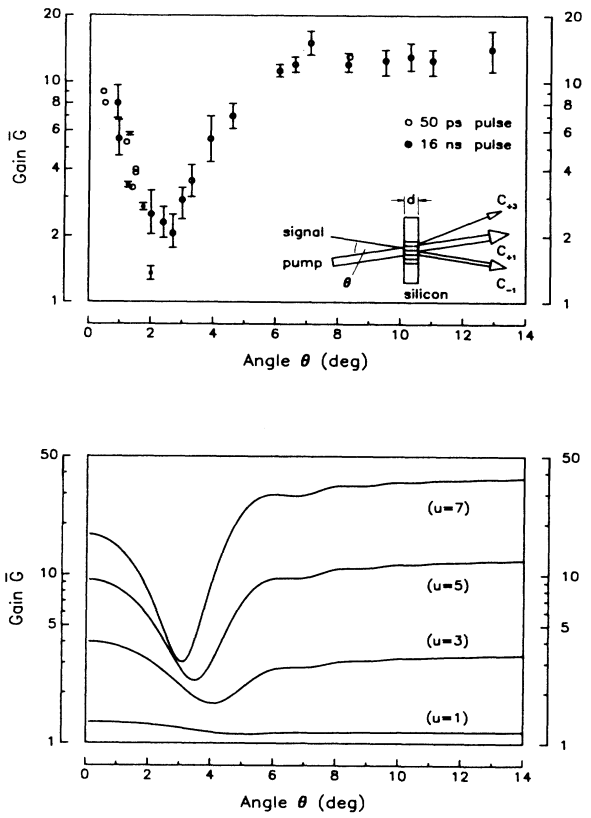

FIG. 1. (a) Experimental maximum gain as a function of beam intersection angle θ for ns pulses (low-transmission sample as in Fig. 3) and ps pulses (same sample as in Fig. 2). (b) Calculated gain as a function of angle θ for different pump energy densities.

EXPERIMENTS

The experimental setup is sketched in Fig. 1(a). A pulsed Nd:YAG laser (where YAG represents yttrium aluminum garnet) with active and passive mode locking was used to produce a train of pulses. A single pulse [$t_p = 50$ ps full width at half maximum (FWHM)] was selected with an electro-optic shutter and amplified by two Nd:YAG amplifiers, resulting in a maximum output energy of 10 mJ. The beam was split with a semitransparent mirror into the signal and pump which intersected in the silicon samples. The optical delay of the two pulses was adjusted to be much smaller than the coherence length. The signal beam energy incident on the sample was about 1 mJ/cm^2, whereas pump energy densities up to 300 mJ/cm^2 were used, which is near the damage threshold of silicon. Experiments have been performed also with a Q-switched Nd:YAG laser (16-ns FWHM pulse width). The silicon samples had (100) or (111) orientation and were polished on both sides. Samples with thickness $d = 0.4$, 0.5, and 1.0 mm were used with absorption coefficients $\alpha = 10$ cm^{-1} (weakly p doped, $\rho > 10$ Ω cm) and $\alpha' = 26$ cm^{-1} (heavily n doped, $\rho \approx 0.01$ Ω cm).

The gain $\bar{G}$ is defined as the ratio of the signal beam energies measured behind the silicon crystal with incident and blocked pump. The net gain $T_i\bar{G}$, defined as the ratio of the signal energies behind and in front of the pumped crystal, is obtained by multiplication with the transmission T_i which amounted to 30% for the undoped ($d = 0.4$ mm) and 13% for the doped sample ($d = 0.5$ mm).

The dependence of the gain on the pump energy density is shown in Fig. 2 measured with picosecond pulses. A maximum gain $G = 14$ is obtained at 100 mJ/cm^2 pump energy density and a beam intersection angle $\theta = 8.3°$. The saturation and decrease of the gain at higher energies will be discussed later. The dependence of the maximum gain on the beam intersection angle is shown in Fig. 1(a). This gain has a pronounced minimum at an angle of 2.5°–3°. This minimum is due to a change from a three-wave-mixing process to two-wave mixing (theory, see below). At small angles a third weak beam is visible behind the sample which is produced by diffraction of the bump beam into a direction opposite the signal beam. At large angles $\theta > 5°$, the third beam is not visible or very weak because it is not phase matched, as will be discussed later.

With longer pulses (16 ns), gain is only observed up to angles of 2°, i.e., in the three-wave-mixing regime. The grating decay time is calculated from Eq. (5) to $\tau_2 = 24$ ns at $\theta = 2°$. For larger angles, two-wave mixing has to be considered. However, the grating decay time τ_2 becomes then smaller than the pulse width and therefore amplification does not take place anymore.[1] The initial decrease of the gain with increasing angles θ is about the same for picosecond and nanosecond pulses. It can be assumed therefore that this decrease and the following minimum in the gain curve is not caused by a changing ratio t_p/τ_2 but by the change from three-wave mixing to a two-wave process.

In Figs. 3 and 4, the dependence of the gain for nanosecond pulses is shown for silicon samples with different doping and different temperatures. Samples with low doping and small absorption ($\alpha = 10$ cm^{-1}) give a much higher net gain, $T_i\bar{G}$. Doping leads to free-carrier absorption (intraband transitions), whereas the initial absorption is due to interband transitions resulting in free-carrier production. This is necessary to obtain gain. Doping results only in linear loss, so that $T_i\bar{G}$ is smaller than in undoped samples. The interband absorption can be changed with temperature (Fig. 4). Low temperature results in low absorption so that higher pump energies are needed to obtain gain.

All experiments were performed with energy densities in the range from 1–300 mJ/cm^2. The maximum pulse amplifications were observed at 100 mJ/cm^2 energy density. Above 300 mJ/cm^2, surface damage takes place. The densities of generated electron-hole pairs are in the order of 10^{18} cm^{-3}.

Interaction of laser pulses with silicon has been studied extensively also in the context of laser annealing.[10,11]

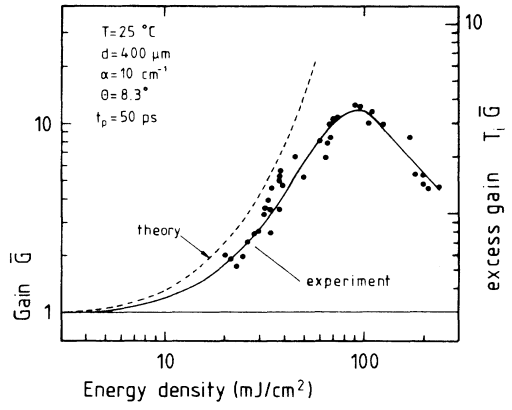

FIG. 2. Two-wave-mixing gain as a function of pump energy density measured with picosecond pulses ($t_p = 50$ ps). The dashed curve is calculated from Eq. (12).

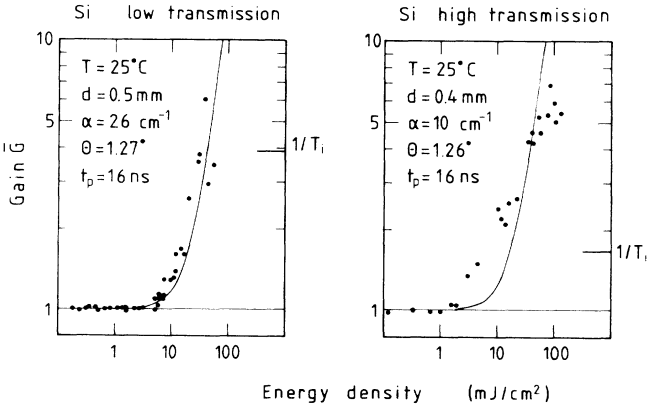

FIG. 3. Three-wave-mixing gain as a function of pump energy density for high- and low-transmission samples ($t_p = 16$ ns). The solid curves are calculated from Eq. (20).

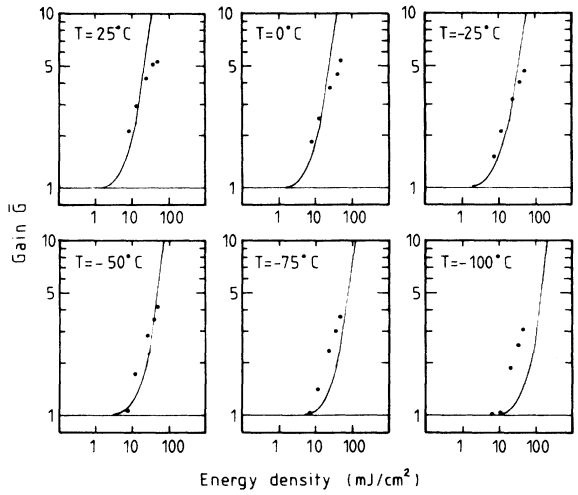

FIG. 4. Temperature dependence of three-wave-mixing gain for a high-transmission sample ($d=1$ mm, $\theta=1°$, $t_p=16$ ns). Solid curves show calculation using Eq. (20).

Pulse energy densities of 0.1—5 J/cm^2 are used for this purpose, resulting in plasma densities up to 10^{20} cm^{-3}; much larger than in our experiment. Therefore, high density effects, e.g., Auger recombination, which are important in laser annealing are of minor importance here. The optical absorption of silicon amounts to some 10 cm^{-1} so that carriers are excited over the total thickness of the crystal in contrast to laser annealing where carriers are produced only in a thin surface layer. Therefore, surface recombination is not considered in the present paper.

THEORY: BASIC EQUATIONS

The amplitudes of the incident signal and pump waves are denoted with C_{-1} and C_{+1}, respectively. The amplitudes C_m of the mth-order diffracted beams are determined by[1]

$$\frac{1}{v}\frac{\partial C_m}{\partial t}-\frac{i}{2k_z}\frac{\partial^2 C_m}{\partial z^2}+\frac{\partial C_m}{\partial z}+\frac{ik_x^2}{2k_z}(m^2-1)C_m+\frac{\alpha}{2}C_m = ik_{e\text{-}h}\sum_{L=-\infty}^{\infty}N_L C_{m-L} . \quad (1)$$

The Lth spatial Fourier component of the charge carrier density grating is given by

$$\frac{\partial N_L}{\partial t}=\kappa\sum_{m=-\infty}^{\infty}C_m C_{m-L}^{*}-\frac{N_L}{\tau_L} . \quad (2)$$

Here, θ is the beam intersection angle outside the sample, θ' the intersection angle in the sample, k_0 the vacuum wave vector,

$$k_x=k_0\sin\frac{\theta}{2},\quad k_z=nk_0\cos\frac{\theta'}{2},\quad v=\frac{ck_z}{n^2k_0} . \quad (3)$$

$n=3.56$ is the refractive index of silicon. The coupling parameters are defined as

$$\kappa=\frac{\alpha}{h\nu},\quad k_{e\text{-}h}=\frac{k_0^2 n n_{e\text{-}h}}{k_z} , \quad (4)$$

where α is the interband absorption coefficient (10 cm^{-1} at room temperature) and $n_{e\text{-}h}=-10^{-21}$ cm^3 is the dispersion volume of the electron-hole pairs.[12] The grating decay times τ_L are given by

$$\tau_L^{-1}=\tau_{e\text{-}h}^{-1}+D_a k_x^2 L^2 , \quad (5)$$

where $\tau_{e\text{-}h}$ is the carrier lifetime and $D_a=10$ cm^2/s is the ambipolar diffusion coefficient. For our experiments, carrier recombination is negligible ($\tau_{e\text{-}h}\to\infty$).

Because of the inversion symmetry of the silicon crystal, all amplitudes $C_m=0$ for $m=0,\pm2,\pm4,\ldots$. If the phase grating modulation induced by C_{+1} and C_{-1} is small compared to 1 (as in the experiments described here), only one additional diffracted beam with amplitude C_{+3} has to be considered. Hence, the general equations (1) and (2) reduce to

$$\begin{aligned}&\frac{\partial C_{+3}}{\partial Z}+\frac{4ik_x^3}{k_z}C_{+3}=ik_{e\text{-}h}N_2C_{+1}-\frac{\alpha}{2}C_{+3} ,\\ &\frac{\partial C_{-1}}{\partial Z}=ik_{e\text{-}h}N_2^{*}C_{+1}-\frac{\alpha}{2}C_{-1} ,\\ &\frac{\partial N_2}{\partial t}+\frac{N_2}{\tau}=\kappa(C_{+3}C_{+1}^{*}+C_{+1}C_{-1}^{*}) .\end{aligned} \quad (6)$$

The pump beam amplitude C_{+1} is considered to change only by absorption. τ is written instead of τ_2 and $Z=z+vt$. The phase shift due to N_0 is included in the amplitudes C_m. In addition, the second-order derivatives are neglected.

TWO-WAVE MIXING

For large beam intersection angles $\theta\gg\theta_0$, the additional third beam C_{+3} is quenched by interference. θ_0 may be calculated from

$$4k_{x,0}^2\,d/k_z=\pi,\quad k_{x,0}=k_0\sin\frac{\theta_0}{2} . \quad (7)$$

For example, $d=0.4$ mm, $\lambda=1.064$ μm yield, $\theta_0=3.9°$, which is of the order of the minimum gain angle in Fig. 1(a). To solve Eq. (6) with $C_{+3}=0$, rectangular incident pulses are assumed, i.e., $C_{\pm1}(z=0,t)=C_{\pm1}(0)$, $0\le t\le t_p$. An analytic solution is obtained for small signal gain, where $C_{+1}(z,t)=C_{+1}(0)$ is assumed. Pump wave absorption is discussed later. One obtains with these assumptions

$$\frac{\partial^2 C_{-1}}{\partial z\,\partial t}=i\kappa k_{e\text{-}h}\,|C_{+1}|^2C_{-1}-\frac{1}{\tau}\frac{\partial C_{-1}}{\partial z}-\frac{\alpha}{2}\frac{\partial C_{-1}}{\partial t} . \quad (8)$$

Here, Z is replaced by z, since in the experiments described here $vt_p/d\gg1$. This means, that the time derivative in Eq. (1) may be ignored. For the present, the first-order derivatives in Eq. (8) are neglected, i.e., $\tau\to\infty$, $\alpha=0$. The influence of grating decay and signal wave ab-

sorption is discussed below.

Introducing the variable

$$u=u(z,t)=(-4\kappa k_{e\text{-}h}\,|\,C_{+1}\,|^2 zt)^{1/2}\,, \tag{9}$$

Eq. (8) reduces to the ordinary differential equation

$$\left[u\frac{d^2}{du^2}+\frac{d}{du}+iu\right]C_{-1}(u)=0,\quad \alpha=0,\quad \tau=\infty\,. \tag{10}$$

The solution is given by Kelvin functions ber and bei:[13]

$$C_{-1}(z,t)=C_{-1}(0)[\mathrm{ber}(u)-i\,\mathrm{bei}(u)]\,,\alpha=0,\ \tau=\infty$$
$$=C_{-1}(0)[1-iu^2/4-u^4/64+iu^6/2304+\cdots]\,. \tag{11}$$

The energy gain experimentally determined is calculated as

$$\bar{G}=\frac{1}{|\,C_{-1}(0)\,|^2 t_p}\int_0^{t_p}|\,C_{-1}(d,t)\,|^2 dt$$
$$=\frac{2}{w}[\mathrm{ber}(w)\mathrm{bei}'(w)-\mathrm{ber}'(w)\mathrm{bei}(w)]\,,$$
$$\alpha=0,\quad \tau=\infty\,, \tag{12}$$

where $w=u(d,t_p)$. This theoretical dependence is shown in Fig. 2, together with picosecond experimental results. The experimental gain is smaller than the theoretical one at a given pump energy density. This can be explained with pump wave absorption, as discussed below.

Grating decay and signal wave absorption are considered now by taking into account the first-order derivatives in Eq. (8). Using the Riemann integration method[14,15] the following result is obtained:

$$C_{-1}(z,t)=C_{-1}(0)e^{-\alpha z/2}\left[\{\mathrm{ber}[u(z,t)]-i\,\mathrm{bei}[u(z,t')]\}e^{-t/\tau}+\frac{1}{\tau}\int_{t'=0}^{t}\mathrm{bei}[u(z,t')]e^{-t'/\tau}dt'\right.$$
$$\left.-\frac{i}{\tau}\int_{t'=0}^{t}\mathrm{bei}[u(z,t')]e^{-t'/\tau}dt'\right]. \tag{13}$$

If linear pump wave absorption is taken into account, then $|\,C_{+1}\,|^2$ is replaced by $|\,C_{+1}(0)\,|^2 e^{-\alpha z}$ in Eq. (8). In this case, u must be replaced by[15]

$$\tilde{u}(z,t)=[-4\kappa k_{e\text{-}h}\,|\,C_{+1}(0)\,|^2 t(1-e^{-\alpha z})/\alpha]^{1/2}\,. \tag{14}$$

This correction applies for Eqs. (11), (12), and (13). For $\alpha=10\ \mathrm{cm}^{-1}$ and $d=0.4$ mm, one obtains $(1-e^{-\alpha d})/\alpha=0.82d$. This explains quantitatively the difference between experimental and theoretical curves in Fig. 2 up to 40 mJ/cm^2. Above 40 mJ/cm^2 the two-wave-mixing gain is expected to be influenced also by nonlinear pump wave absorption. At $E=40$ mJ/cm^2 the carrier concentration is $N=\kappa E=2\times10^{18}\ \mathrm{cm}^{-3}$. Since the free-carrier cross section is $\sigma_{e\text{-}h}=5\times10^{-18}$ cm^2,[16] the total absorption coefficient is $\alpha''=\alpha+\sigma_{e\text{-}h}\times N=20\ \mathrm{cm}^{-1}$.

The saturation and decrease of the gain at high pump energies is explained as follows. The carrier density saturates at high pump energy densities because of free-carrier absorption. The free-carrier grating results from a small spatial modulation from the pump energy density. The amplitude of the grating therefore decreases if the total carrier density saturates. The decreasing grating amplitude causes a reduction of the gain. In addition, the gain is reduced by the decreasing transmission of the silicon crystal. A detailed theoretical description of the reduction of the grating amplitude and transmission at high pump energies has been worked out for evaluation of a four-wave-mixing (FWM) experiment in silicon.[17] Maximum FWM reflectivity was obtained experimentally and theoretically at a pump energy density of about 100 mJ/cm^2, the same value giving maximum gain. FWM reflectivity and the two-wave-mixing gain are explained by a similar grating mechanism. We conclude therefore that also the gain maximum is explained by the same mechanism as the FWM maximum: free-carrier absorption.

For $t=\infty$ the integrals in Eq. (13) can be evaluated[18]

$$C_{-1}(z,t=\infty)=C_{-1}(0)\exp[-\alpha z/2-iu^2(z,\tau)/4]\,, \tag{15}$$

which shows that no gain is obtained for cw signal and pump waves. On the other hand, for $\tau=\infty$ or short pump and signal pulses, Eq. (13) results in Eq. (11) if gain is defined with respect to the unamplified transmitted signal energy.

Results of some numerical evaluation of Eq. (13) are shown in Fig. 5. The experiments described in this paper satisfy $u<7.5$. The integrals appearing in (13) were calculated numerically. Pump and signal wave absorption is neglected. The intensity gain curves with $u(z,t_p)=\mathrm{const}$ are approximately straight lines. This means an exponential dependence of the intensity gain from t_p/τ for constant pump energy density. Therefore, the following approximation may be used to calculate the intensity gain $|\,C_{-1}(z,t_p;\tau)/C_{-1}(0)\,|^2$:

$$\left|\frac{C_{-1}(z,t)}{C_{-1}(0)}\right|^2-1\simeq\{\mathrm{ber}^2[u(z,t)]+\mathrm{bei}^2[u(z,t)]-1\}$$
$$\times\exp\{-[1.3+0.004u^2(z,t)]t/\tau\}\,,$$
$$t=t_p\,. \tag{16}$$

Since t_p is fixed in our experiments a variation of t_p/τ means a variation of the beam intersection angle according to Eq. (5). The solid lines in Fig. 5 thus demonstrate the angular dependence of two-wave-mixing gain.

The maximum beam intersection angle for which pi-

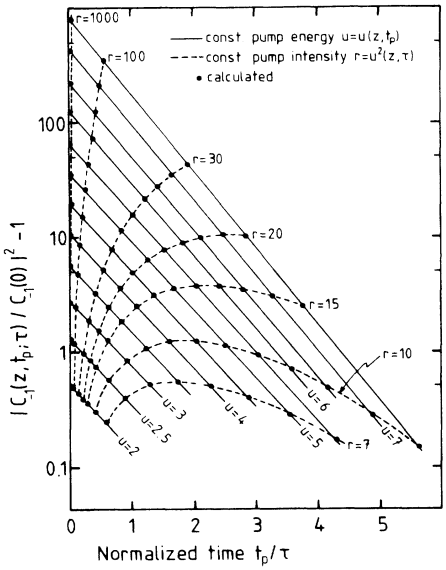

FIG. 5. Calculated intensity gain as a function of normalized time t_p/τ. The solid lines show the dependence on reciprocal grating decay time τ with constant pump pulse width t_p and energy density. The dashed lines demonstrate the dependence on pulse width t_p with constant pump intensity and fixed grating decay time τ.

cosecond pulse amplification can be obtained is estimated from $t_p/\tau=0.5$, $t_p=50$ ps to be $\theta=30°$.

The dashed lines $r=u^2(z,\tau)=$const in Fig. 5 show the intensity gain at time t_p with fixed pump intensity and fixed grating decay time. According to Eq. (12) the energy gain $\bar{G}$ is the time average of the intensity gain.

THREE-WAVE MIXING

If the beam intersection angle θ is sufficiently small, the dephasing term in Eq. (6) can be neglected. Again assuming rectangular pulses and $C_{+1}(z,t)=C_{+1}(0)\exp(-\alpha z/2)$, one obtains

$$\frac{\partial^2 N_2}{\partial t\,\partial z}=-\frac{1}{\tau}\frac{\partial N_2}{\partial z}-\alpha\frac{\partial N_2}{\partial t}-\frac{\alpha}{\tau}N_2\ , \tag{17}$$

resulting in

$$N_2(z,t)=\kappa C_{+1}(0)C^*_{-1}(0)e^{-\alpha z}\tau(1-e^{-t/\tau}) \tag{18}$$

and

$$C_{-1}(z,t)=C_{-1}(0)e^{-\alpha z/2}\left[1-\frac{i}{4}\tilde{u}^2(z,\tau)(1-e^{-t/\tau})\right]\ . \tag{19}$$

This equation predicts that gain is possible in the three-wave-mixing regime also with long pulses or even with continuous waves.

It should be remembered that no cw gain is obtainable with two-wave mixing. The energy gain is obtained as

$$\bar{G}-1=\frac{\tilde{u}^4(d,\tau)}{16}\frac{\tau}{t_p}\left[\frac{t_p}{\tau}-\tfrac{3}{2}+2e^{-t_p/\tau}-\tfrac{1}{2}e^{-2t_p/\tau}\right]\ . \tag{20}$$

Dependences of the gain on the pump energy calculated from Eq. (20) in comparison with experimental results are shown in Figs. 3 and 4. For low-transmission samples, interband absorption [for calculating κ from Eq. (4)] has to be distinguished from total absorption [for calculating u from Eq. (14)]. The interband absorption amounts to 10 cm^{-1} at $T=25$ °C. The total absorption is specified in Fig. 3. The heavily doped sample (low transmission) exhibits good agreement between theory and experiments, whereas the high-transmission sample gives an experimental gain which is larger than expected from theory at low pump energies. The temperature dependence of α for the calculation shown in Fig. 4 has been taken from Ref. 19. Calculated and experimental values in Fig. 4 agree at $+25$ to -25 °C, whereas the experimental gain becomes larger than that calculated at low temperature. This can be possibly explained by a temperature change of $n_{e\text{-}h}$.

TRANSITION BETWEEN TWO- AND THREE-WAVE MIXING

To describe the transition from three-wave mixing to two-wave mixing, the dephasing term in Eq. (6) must be taken into account. The following perturbation calculation is simplified by neglecting absorption and grating decay, i.e., the following equations are used instead of (6):

$$\frac{\partial C_{+3}}{\partial z}+iAC_{+3}=ik_{e\text{-}h}C_{+1}N_2\ ,$$
$$\frac{\partial C_{-1}}{\partial z}=ik_{e\text{-}h}C_{+1}N_2^*\ , \tag{21}$$

and

$$\frac{\partial N_2}{\partial t}=\kappa(C_{+3}C^*_{+1}+C_{+1}C^*_{-1})\ . \tag{22}$$

$A=4k_x^2/k_z$ is a function of the beam intersection angle θ according to Eq. (3).

A first approximation for N_2 may be calculated from (22) by replacing all wave amplitudes by their values at $z=0$ (given field approximation):

$$N_2^{(1)}=\kappa\int(C^{(0)}_{+3}C^*_{+1}+C_{+1}C^{(0)*}_{-1})dt=\kappa C_{+1}C^{(0)}_{-1}t\ . \tag{23}$$

Equation (23) is valid since the zeroth-order approximations of C_{+3} and C_{-1} are given by $C^{(0)}_{+3}=0$, $C^{(0)}_{-1}=C_{-1}(0)$. As before, $C_{-1}(0)$ is the amplitude of the incident rectangular signal pulse. C_{+1} is regarded as constant.

Replacing N_2 by $N_2^{(1)}$ on the right-hand side of Eqs. (21), these can be solved to give the first approximations for C_{+3} and C_{-1}:

$$C_{-1}^{(1)}=C_{-1}(0)\left[1-\frac{i}{4}u^2(z,t)\right],$$
$$C_{+3}^{(1)}=\frac{\kappa k_{e\text{-}h}}{A}C_{+1}^2C_{-1}^*(0)t(1-e^{-iAz}). \quad (24)$$

This result can be used on the right-hand side of Eq. (22) to determine the second-order approximation for N_2, which allows the calculation of the second-order approximation for the signal wave amplitude:

$$C_{-1}^{(2)}=C_{-1}(0)\left\{1-\frac{iu^2}{4}\left[1-i\frac{u^2}{16}-\frac{u^2}{8A}\left[1+\frac{i}{Az}(e^{iAz}-1)\right]\right]\right\}. \quad (25)$$

For the Bragg condition, Eq. (25) yields

$$C_{-1}^{(2)}=C_{-1}(0)\left[1-\frac{iu^2}{4}-\frac{u^2}{64}\right],\quad Az\gg 1. \quad (26)$$

This means that the first three terms of the exact solution (11) for two-wave mixing are reproduced. On the other hand, from small θ, Eq. (25) results in

$$C_{-1}^{(2)}=C_{-1}(0)\left[1-i\frac{u^2}{4}\right],\quad Az\ll 1. \quad (27)$$

This is the exact result, Eq. (19), for $\alpha=0$ and $\tau=\infty$.

For comparison with experimental results, the second-order approximation for the gain must be calculated:

$$\bar{G}=\frac{1}{|C_{-1}(0)|^2t_p}\int_0^{t_p}|C_{-1}^{(2)}(d,t)|^2dt. \quad (28)$$

Equation (28) is easily evaluated since u^2 is proportional to t, according to Eq. (9). The result of the elementary integration is not given here explicitly. In Fig. 1(b) numerical values of the gain $\bar{G}$ are given as a function of the beam intersection angle for $u(d,t_p)=1$, 3, 5, and 7. It should be noted that a maximum instead of a minimum would be obtained in Fig. 1(b) if $n_{e\text{-}h}$ were not negative. For the experimental data shown in Fig. 1(a), $u=7$ is valid. Comparison of the corresponding curve in Fig. 1(b) with the experimental curve in Fig. 1(a) shows that experiment and theory give about the same minimum gain angle at 2.5°–3°. The calculated gain values are larger than the measured one because of free-carrier absorption, as discussed above. Another reason for this deviation is given by the approximations used in the calculations.

SUMMARY

Energy transfer from strong pump beams to weak signal beams crossing in silicon samples has been investigated. This leads to amplification of picosecond pulses with a gain up to 20. At small intersection angles the interaction is described as a three-wave-mixing process, whereas at larger angles, two-wave mixing is important. At intermediate angles of 2°–3° a sharp decrease of the gain is observed.

The fast energy transfer process in silicon may have applications not only for signal amplification but for beam switching, modulation, and deflection. Further work is necessary to optimize the transfer efficiency.

ACKNOWLEDGMENT

The research was supported by the Deutsche Forschungsgemeinshaft (DFG).

*Permanent address: Physical Department, Technical University of Harbin, Peking, Harbin, Heilongjing, People's Republic of China.

[1]V. L. Vinetskii, N. V. Kukhtarev, S. G. Odulov, and M. S. Soskin, Usp. Fiz. Nauk. **129**, 113 (1979) [Sov. Phys.—Usp. **22**, 742 (1979)].

[2]H. J. Eichler, P. Günter, and D. Pohl, *Laser-Induced Dynamics Gratings*, Vol. 5 of *Springer Series in Optical Science* (Springer-Verlag, Berlin, 1986).

[3]F. Laeri, T. Tschudi, and J. Albers, Opt. Commun. **47**, 347 (1983).

[4]A. Krumins and P. Günter, Appl. Phys. **19**, 153 (1979).

[5]V. L. Vinetskii, T. E. Zaporozhets, N. V. Kukhtarev, A. S. Matviichuk, S. G. Odulov, and M. S. Soskin, Pis'ma Zh. Eksp. Teor. Fiz. **25**, 432 (1977) [JETP Lett. **25**, 404 (1977)].

[6]V. L. Vinetskii, N. V. Kukhtarev, and M. S. Soskin, Kvant. Elektron. (Moscow) **4**, 420 (1977) [Sov. J. Quantum. Electron. **7**, 230 (1977)].

[7]K. Jarasiunas and H. J. Gerritsen, Appl. Phys. Lett. **33**, 190 (1978).

[8]A. A. Borshch, M. S. Brodin, V. I. Volkov, V. V. Ovchar, and D. T. Tarashchenko, Kvant. Elektron. (Moscow) **4**, 646 (1977) [Sov. J. Quantum Electron. **7**, 358 (1977)].

[9]H. J. Eichler and F. Massmann, J. Appl. Phys. **53**, 3237 (1982).

[10]H. M. Van Driel, *Semiconductors Probed by Ultrafast Laser Spectroscopy*, edited by R. R. Alfano (Academic, New York, 1984), Vol. II, p. 57ff.

[11]K. Murakami, *Semiconductors Probed by Ultrafast Laser Spectroscopy*, edited by R. R. Alfano (Academic, New York, 1984), Vol. II, p. 171ff.

[12]J. P. Woerdman, Phillips Res. Suppl. **7**, 1 (1971).

[13]M. Abramowitz and I. A. Stegun, *Handbook of Mathematical Functions*, 9th ed. (Dover, New York).

[14]L. Solymar and J. M. Heaton, Opt. Commun. **51**, 76 (1984).

[15]H. M. Lieberstein, *Theory of Partial Differential Equations* (Academic, New York, 1972).

[16]T. F. Bogges, K. M. Bohnert, K. Mansur, S. C. Moss, I. W. Boyd, and A. L. Smirl, IEEE J. Quantum Electron. **QE-22**, 360 (1986).

[17]H. J. Eichler, J. Chen, and K. Richter, Appl. Phys. (to be published).

[18]I. S. Gradstein and I. M. Ryshik, *Tables of Series, Products and Integrals* (Harri Deutsch, Thun-Frankfurt M., 1981), Vol. 2. Formulas 6.872.3/4 are used.

[19]G. G. MacFarlane, T. P. McLean, J. E. Quarrington, and V. Roberts, Phys. Rev. **111**, 1245 (1958).